

EXPERIMENTAL STUDY OF DEVELOPING TURBULENT FLOW AND HEAT TRANSFER IN RIBBED CONVERGENT/DIVERGENT RECTANGULAR DUCTS

by

**Sivakumar KARTHIKEYAN^{a*}, Natarajan ELUMALAI^b,
and Kulasekharan NARASINGAMURTHI^c**

^a Department of Mechanical Engineering, Valliammai Engineering College, Chennai, India

^b Institute for Energy Studies, Anna University, Chennai, India

^c Department of Mechanical Engineering, Saveetha Engineering College, Chennai, India

Original scientific paper

DOI: 10.2298/TSCI140107100K

The article represents an experimental investigation of friction and heat transfer characteristics of divergent/convergent rectangular ducts with an inclination angle of 1° in the y-axis. Measurements were taken for a convergent/divergent rectangular duct of aspect ratio at inlet 1.25 and outlet in convergent channel 1.35; but in case of divergent duct it can be reversed. The four uniform rib heights, $e = 3, 6, 9,$ and 12 mm the ratio between rib height to hydraulic mean diameter are 34.8, 69.7, 104.6, and 138.7, a constant rib pitch distance, $P = 60$ mm has been used. The flow rate in terms of average Reynolds number based on the hydraulic mean diameter is 86 mm of the channel was in a range of 20,000 to 50,000. The two ceramic heating strip of 10 mm thickness is used as a heating element have attached on top and bottom surfaces for the test sections. The heat transfer performance of the divergent/convergent ducts for 3, 6, 9, and 12 mm ribs was conducted under identical mass flow rate based on the Reynolds number. In our experiments has totally 8 different ducts were used. In addition, the acceleration/deceleration caused by the cross-section area, the divergent duct generally shows enhanced heat transfer behavior for four different rib sizes, while the convergent duct has an appreciable reduction in heat transfer performance. From result point view divergent duct with 3 mm height ribbed square duct gets maximum heat transfer coefficient with minimum friction loss over the other convergent/divergent ducts.

Key words: *convergent/divergent duct, rib turbulators, Nusselt number, friction factor*

Introduction

Among the various engineering applications involving heat transfer augmentation in cooling passages, the repeated surface ribs are often treated as turbulence promoters to enhance heat transfer. Internal cooling is applied in gas turbines blades to allow maximum inlet temperatures, so as to make high thrust/weight ratios and low specific fuel consumption. The rotor inlet temperatures (RIT) in gas turbine, in many practical cases, are far higher than the allowable temperature of the blade material; therefore turbine blades need to be cooled. The blades are cooled by extracted air from the compressor of the engine. Since this extraction in-

* Corresponding author; e-mail: tjksiva2k@yahoo.co.in

curs a penalty to the thermal efficiency, it is to understand and optimize the cooling technique, operating conditions, and turbine blade geometry. Gas turbine blades can be either cooled internally or externally.

Turbulent heat transfer and fluid flow characteristics of air in rib-roughened tubes, ducts and between parallel plates have been studied extensively because of their important applications. Such a heat transfer enhancement method is widely used in cooling passages of gas turbine blade, compact heat exchangers, fuel elements in advanced gas-cooled reactor electronic cooling devices, *etc.* Taking the cooling passages is usually approximated by a rectangular duct with a pair of opposite rib-roughened walls. In the computational investigations reported in the literature, the internal cooling passages of a gas turbine have been modelled by either square or rectangular channels having two ways. As presented by Abuaf and Kercher [1] in typical airfoils with multipass cooling circuits, the cross-sectional area of radial passage usually varies along the passage from root to tip. In other words, the cooling passages are actually convergent to some extent. Such a geometric variation may induce substantial difference in both flow and heat transfer characteristics compared to those models with straight rectangular channel.

A large number of experimental studies are reported in the literature on internal cooling in turbine blade passages, particularly for square coolant passages [2-7]. Most of the earlier computational studies on internal cooling passage of the blades have been restricted to three-dimensional steady RANS simulations [8, 9]. Sivakumar *et al.* [10] did an experimental comparison between smooth and different sized rib with the divergent rectangular ducts in heat transfer and pressure drop. Sivakumar *et al.* [11] conducted in convergent rectangular duct with heat transfer and friction factor for various ribs height. The flow and heat transfer through a two pass smooth and 45° rib roughened rectangular duct with an aspect ratio of 2 has been reported by Qantani *et al.* [12] using Reynolds stress turbulence model. They have found reasonable agreement with experimental studies however, in certain regions there were some significant discrepancies. However, no significant study has been found in the existing literature that deals with heat transfer in ribbed roughened convergent ducts. Wang *et al.* [13] found that for a smooth square duct a mild streamwise variation of cross-sectional area may induce significant difference in the local and average heat transfer behaviours. Rongguang *et al.* [14] carried out numerical simulation by a multi-block 3-D solver, which is based on solving the Navier-Stokes and energy equation in conjunction with a low-Reynolds number $k-\omega$ turbulence model. Chandra *et al.* [15] conducted an experimental study of surface heat transfer and friction characteristics of a fully developed turbulent air flow in a square channel with transverse ribs on one, two three and four walls is reported, similar way triangular channel with a rounded edge as a model of a leading edge cooling for a gas turbine blade was presented by experimentally Amro *et al.* [16]. Abhishek *et al.* [17] presented local heat transfer distributions in a double wall ribbed square channel with 90° continuous, 90° saw tooth profiled and 60° V-broken ribs. Comparable heat transfer enhancements caused by 60° V-broken ribs are higher than others.

An experimental investigation on turbulent heat transfer and friction loss behaviors of airflow through a constant heat-fluxed channel fitted with different heights of triangular ribs was conducted by Thianpong *et al.* [18] with $AR = 10$ and height $H = 30$ mm with three uniform rib heights, $e = 4, 6,$ and 8 mm, and one non-uniform rib height $e = 4$ mm and 6 mm, alternately, for a single rib pitch $p = 40$ mm. Comparatively the uniform rib height performs better than the corresponding non-uniform one. Nine *et al.* [19] conducted an experiment and numerical analysis in a rectangular channel with semicircular ribs with uniform height 3 mm and 5 mm on one

wall with four different rib pitches 28, 35, 42, and 49 mm turbulence and pressure drop behaviors. Friction factor is greatly influenced by rib pitch to rib height ratio where with increasing the number of P/e ratio decreases additional pressure loss at the same Reynolds number. Caliskan and Baskaya [20] discuss which the heat transfer measurement over a surface with V-shaped ribs and convergent-divergent shaped ribs by a circular impinging jet array was investigated using thermal infrared camera. During the experiments the Reynolds number was varied from 2000 to 10,000. Abdularzraq *et al.* [21] simulated the turbulent heat transfer to fluid flow through channel with triangular ribs of different angles were presented in ANSYS 14 ICEM and ANSYS 14 FLUENT. Sriharsha *et al.* [22] done an experiments to find effect of rib height to the hydraulic diameter ratio on the local heat transfer distribution in a double wall ribbed square channel with 90° continuous attached and 60° V-broken ribs. The effect of detachment of the rib in case of broken ribs on the heat transfer characteristic is also presented. Sjerić *et al.* [23] developed two zone $k-\epsilon$ turbulence models for the cycle-simulation software in internal combustion engines plays the most important role in the combustion process. Bakić *et al.* [24] presented experimental investigation of turbulent structures of flow around a sphere by laser-Doppler anemometry and Reynolds number of 50,000.

From the literature survey, no significant study was found, that deals with the heat transfer in rib roughened rectangular convergent/divergent duct with different sized ribs. Experimental results are presented using four different height rib configurations in to turbulent channel flow under 20,000 to 50,000 Reynolds number. The principle aim of the experiment is to analyze the effect of rib heights on friction and describe the heat transfer characteristics as well as optimize rib height and minimum friction loss.

Experimental set-up

An experimental set-up has been designed and fabricated to study the effect of the rib's height on the heat transfer and fluid characteristics of air flow in a convergent/divergent rectangular channel. The schematic diagram of an experimental set-up is shown in fig. 1. The system consists of an entry section, test section, exit section, a flow measuring orifice plate with a U-tube manometer, pressure measuring U-tube manometer and a centrifugal blower with a variable regulator to control the blower speed. The copper convergent/divergent rectangular channel tapers with 1:100 inclinations along the length wise direction. The length 300 mm of the test duct is three times the test section width 100 mm. The dimensions of the rectangular duct at entrance section are 100×80 mm and at the exit section 100×74 mm, respectively. The geometry parameters of the test section are mentioned as shown in tab. 1. Test section made up off copper material with 5 mm thickness. Two electrical heaters of size

Figure 1. Schematic experimental set-up
 1 – main plug, 2 – temperature indicator,
 3 – heating coil, 4 – test section with
 thermocouples, 5 – honey comb air
 regulator, 6 – orifice plate, 7 – U-tube
 manometer, 8 – blower ON/OFF switches,
 9 – variable regulator to blower,
 10 – air hose from blower to test section,
 11 – variable speed blower

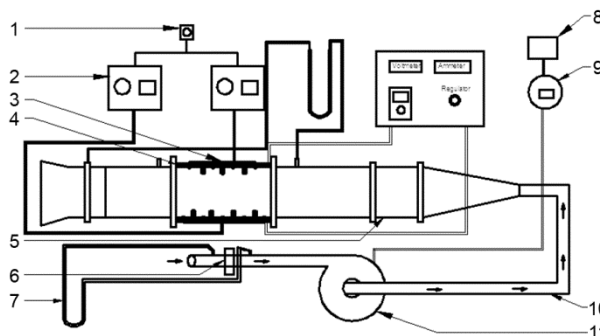


Table 1. Geometry parameters of the test section

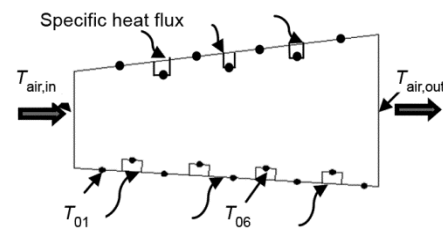
Section	W	e	H	W/H	e/D_m	P/e	Re
Inlet where convergent or outlet where divergent	100	3	80	1.25	0.345	20	20,000
	100	6	80	1.25	0.694	10	30,000
	100	9	80	1.25	0.1040	6.6	40,000
Outlet (or) inlet	100	–	74	1.35	–	–	–

280 × 90 mm fabricated by combining series and parallel loops of heating wire on a 5 mm asbestos sheet were placed at the top and bottom of the test duct. 100 mm glass wool was applied as insulation on the ambient side of the heater and wound around the test section.

The heat flux can be varied from 0 to 500 W/m² by a variac transformer. The mass flow rate of air is measured by means of a calibrated orifice plate connected with the U-tube manometer, using water as the manometer fluid, and the flow is controlled by the voltage variable regulator to control the blower speed. Four ribs were fabricated at the bottom wall surface (RB₀₁ to RB₀₄). Totally 9 thermocouples were attached to the bottom surface and bottom ribs top surfaces and 7 thermocouples are attached at the top surfaces and top rib surfaces and the ribs along its centerline, to measure the surface temperature.

Two more thermocouples are inserted at the inlet and outlet test sections at the bottom of the heating strip to measure the heat supplied to the test section. The thermocouples were calibrated in advance and their accuracy is estimated to be about 0.1 °C. Uncertainty estimation was conducted as suggested by Kline and McClintock [25]. The maximum uncertainty in the average Nusselt number was estimated to be less than 15% and that for the friction factor less than 14%. The pressure drop across the test section was measured by a U-tube manometer having a least count of 0.1 mm. The air is sucked through the rectangular duct by means of a blower driven by a 1-phase, 240 V, 820 W AC. The thermal conductivity of the channel material was about 386 W/mK.

The same dimensional test sectional geometry will be used in the divergent channel; but only in this case the test section will be turned 180° and air will be entered in the reduced inlet section as 100 × 74 mm and leaving through 100 × 80 mm side of the test section as shown in fig. 2.

Figure 2. Divergent channel with temperature measured location

The same dimensional test sectional geometry will be used in the divergent channel; but only in this case the test section will be turned 180° and air will be entered in the reduced inlet section as 100 × 74 mm and leaving through 100 × 80 mm side of the test section as shown in fig. 2.

Experimental procedure

Before starting the experimental investigations, all the thermocouples were checked to measure the same room temperature. The test was conducted under steady-state conditions to collect the relevant heat transfer and flow friction parameters. The steady-state condition was assumed to have been reached, when the temperature at the heating strip did not change for about 50 seconds. When a change in the operating conditions is made, it takes about 2 to 3 hours to reach the steady-state for single Reynolds number. The test was conducted for the Reynolds number range used in between 20·10³ to 50·10³ for every 10,000 increase in Reynolds number. After each change of flow rate, the system was allowed to attain a steady-state condition than that the reading were noted.

The following parameter was measured:

- temperature of the heating strip,
- temperature of the air at the inlet ($T_{\text{air,in}}$) and outlet ($T_{\text{air,out}}$) of the test section,
- temperatures of the ribbed bottom surfaces and top surface temperature of the test section (T_{01} to T_{09} , and T_{10} to T_{16}),
- mass flow across the orifice plate by using the U-tube manometer, and
- pressure difference across the test section by using the U-tube manometer.

The procedure had been repeated for all the rectangular convergent/divergent with various rib heights: (1) 3 mm square rib height channels, (2) 6 mm square rib height channels, (3) 9 mm square rib height channels, and (4) 12 mm square rib height channels.

Data reduction

The local heat transfer coefficient was calculated from the total net heat transfer rate and the different of the local wall temperature and the local bulk mean air temperature from the literature [11] as mentioned in:

$$h_x = \frac{Q - Q_{\text{loss}}}{A(T_{w,x} - T_{b,x})} \quad (1)$$

The local wall temperature used in eq. (1) was read from the output of the thermocouple. The local bulk air temperature of air was calculated by:

$$T_{b,x} = T_{\text{in}} + \frac{(Q - Q_{\text{loss}})A(x)}{Amc_p} \quad (2)$$

where $A(x)$ is the heat transfer surface area from the duct inlet to the position where the local heat transfer coefficient was determined. The heat loss to the environment (Q_{loss}) was estimated by heat conduction through the plastic form and the two end losses. For most of the studied values the ratio of Q_{loss}/Q was less than 5%. This estimation was confirmed by the thermal energy balance between the fluid enthalpy increase and the total power input. In the data reduction (Q_{loss}) was determined from the measured outlet fluid temperature.

The local Nusselt number is defined:

$$\text{Nu}_x = \frac{h_x D_m}{k} \quad (3)$$

The average Nusselt number is defined:

$$\overline{\text{Nu}} = \frac{(Q - Q_{\text{loss}})D_m}{Ak(T_w - T_m)} \quad (4)$$

The characteristic length, the reference temperature and the average wall temperature were determined by eqs. (5) to (7):

$$D_m = \frac{D_{h,\text{in}} + D_{h,\text{out}}}{2} \quad (5)$$

$$T_m = \frac{T_{b,\text{in}} + T_{b,\text{out}}}{2} \quad (6)$$

$$T_w = \frac{1}{A} \int_0^A T_{w,x} dA \quad (7)$$

For most of the cases internal convective heat transfer and fluid properties are evaluated at the mean temperature of the fluid in the duct. The Reynolds number was defined:

$$Re_m = \frac{U_m D_m}{\nu} \quad (8)$$

where U_m is the duct mean cross-sectional average velocity. This is equal to the cross-section average velocity at the duct mid-section.

The friction factor across the entire duct of the uniform cross-section was defined:

$$f = \frac{\frac{\Delta p}{L} D_m}{\frac{\rho U_m^2}{2}} \quad (9)$$

where Δp is the pressure drop of the entire test duct. As for the convergent or divergent duct, the term of pressure loss should be complicated one; it takes the effects of acceleration or deceleration into account from the literature [11].

The average friction factor for the duct is defined:

$$f = \frac{U_{in}^2}{U_m^2} \frac{D_m}{L} \lambda \left[1 - \left(\frac{A_{in}}{A_{out}} \right)^2 \right] \quad (10)$$

where λ and the pressure recovery factors for viscous fluid and for ideal fluid, respectively, defined:

$$\lambda = 1 - \frac{C_p}{C_{p,i}} \quad (11)$$

$$C_p = \frac{P_{out} - P_{in}}{\frac{\rho U_m^2}{2}} \quad (12)$$

$$C_{p,i} = 1 - \left(\frac{A_{in}}{A_{out}} \right)^2 \quad (13)$$

This definition of C_p can be applied for $C_{p,x}$ by replacing p_{out} , p_{in} with $p_x + \Delta x/2$, $p_x - \Delta x/2$, where Δx is the distance between two neighboring pressure taps. In our experiment, the Reynolds number varied from 20,000 to 50,000 and all geometric parameters were kept constant.

Experimental uncertainty

The method described by Moffat [26] was used to estimate the experimental uncertainty. In this study, local Nusselt numbers were determined using eq. (3). The maximum error of the wall temperature T_w by the present method was ± 0.1 °C, and the error of the bulk air temperature was ± 0.1 °C. The heat flux related uncertainty is within $\pm 9\%$. Based on these val-

ues, the uncertainty of the Nusselt number was estimated to be within $\pm 9.2\%$. In the pressure drop test rig, U-tube manometer has an error of less than 1%. The least square fit process yields less than 5% standard deviation in the slope 4 (fRe), according to Box *et al.* [27] If the error induced by the thermal properties and duct dimensions are taken into account in the calculation of the Reynolds number, the friction factor uncertainty was estimated to be within $\pm 8\%$. U-tube manometer with a resolution of 1 mm was used for pressure drop and mass flow rate of air through orifice meter. The inlet air temperature was measured by a thermocouples checked by a thermometer with a resolution of 1 °C.

Results and discussion

In our discussion to simplify the presentation, the following symbols are adopted to present the types of ducts: C-2B – convergent duct with ribbed bottom surface at $Re = 20,000$; C-3B – convergent duct with ribbed bottom surface at $Re = 30,000$; C-4B – convergent duct with ribbed bottom surface at $Re = 40,000$; C-5B – convergent duct with ribbed bottom surface at $Re = 50,000$; D-2B – divergent duct with ribbed bottom surface at $Re = 20,000$, D-3B – divergent duct with ribbed bottom surface at $Re = 30,000$; D-4B – divergent duct with ribbed bottom surface at $Re = 40,000$; and D-5B – divergent duct with ribbed bottom surface at $Re = 50,000$.

Local heat transfers for convergent and divergent channel

The local heat transfer coefficient and friction factor for the ribbed of four different heights 3, 6, 9, and 12 mm in rectangular convergent/divergent rectangular duct for Reynolds number range from 20,000 to 50,000, as shown in figs. 3-10. By a careful examination of these graphs, we may find the following characteristics:

- for all the four different heights rib-roughened ducts, the local heat transfer coefficient increases with the increase in the Reynolds number from 20,000 to 50,000,
- for the ribbed surfaces of the four ducts, the distribution of the local heat transfer coefficient exhibits more or less same periodic pattern after 1-2 ribs for lower Reynolds number. In case of higher Reynolds number, the heat transfer coefficient more significant the periodicity, and
- for the rib-roughened duct of constant cross-section, the heat transfer may be regarded as fully developed after 2-3 ribs, characterizing by almost the same level and variation pattern of the local heat transfer coefficient. Variation of dimensionless distance with heat transfer coefficient for the convergent duct with 20,000 (C-2B) Reynolds number with bottom surface rib attachment as shown in fig. 3. In this figure, heat transfer coefficient for 12 mm rib size is comparatively higher heat transfer enhancement then the other rib sizes in both the bottom surfaces and top rib surfaces of the test sections.

At the same Reynolds number (20,000), the divergent channel (D-2B) shows fig. 4 as 9 mm rib higher heat transfer enhancement then the other rib sizes. Figure 5 shows the variation of dimensionless distance with heat transfer coefficient for the convergent duct with 30,000 (C-3B) Reynolds number with bottom surface rib attachments. From the graph also 12 mm rib height is higher heat transfer enhancement compared to the other rib heights.

Similarly, divergent duct with Reynolds number 30,000 (D-3B) with bottom surface rib attachment shows fig. 6 rib height 9 mm is higher heat transfer enhancement compared to others. Figure 7 shows the variation of dimensionless distance with heat transfer coefficient for the convergent duct with 40,000 (C-4B) Reynolds number with bottom surface rib attachments. From the graph also 12 mm rib height is higher heat transfer enhancement compared to the other rib heights. Similarly divergent duct with Reynolds number 40,000 (D-4B) with

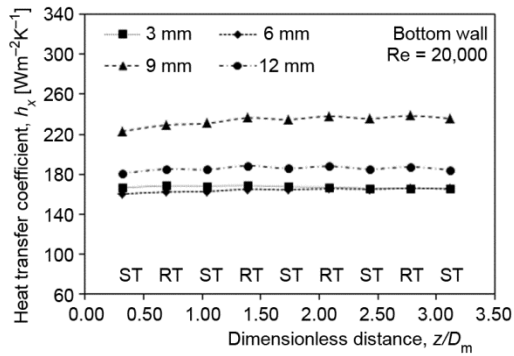


Figure 3. Variation of local heat transfer coefficient for channels with different rib heights, convergent (C-2B)

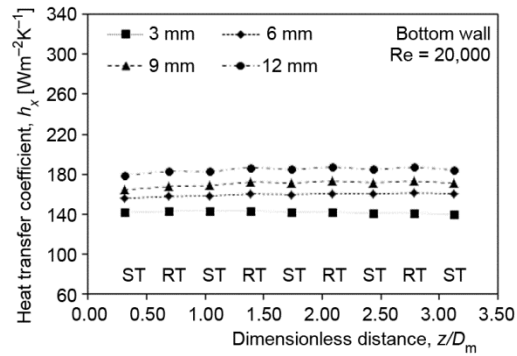


Figure 4. Variation of local heat transfer coefficient for channels with different rib heights, divergent (D-2B)

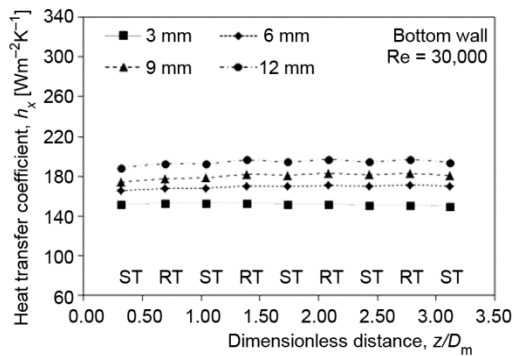


Figure 5. Variation of local heat transfer coefficient for channels with different rib heights, convergent (C-3B)

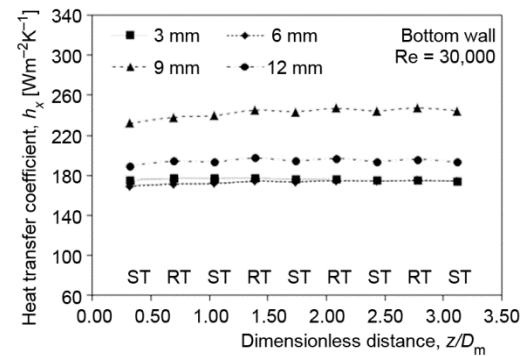


Figure 6. Variation of local heat transfer coefficient for channels with different rib heights, divergent (D-3B)

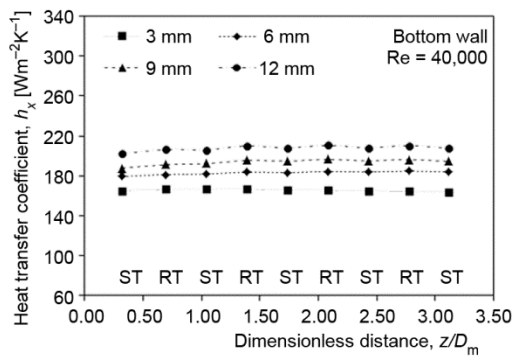


Figure 7. Variation of local heat transfer coefficient for channels with different rib heights, convergent (C-4B)

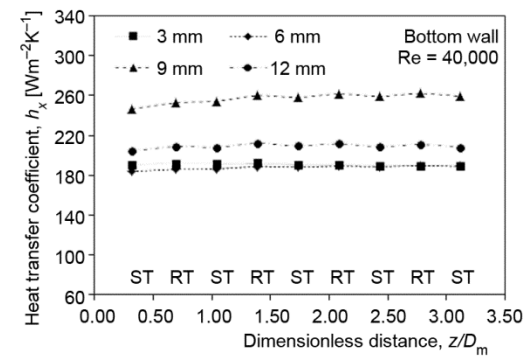


Figure 8. Variation of local heat transfer coefficient for channels with different rib heights, divergent (D-4B)

bottom surface rib attachment shows fig. 8 rib height 9 mm is higher heat transfer enhancement compared to others. Figure 9 shows the variation of dimensionless distance with heat transfer

coefficient for the convergent duct with 50,000 (C-5B) Reynolds number with bottom surface rib attachments. From the graph also 12 mm rib height is higher heat transfer enhancement compared to the other rib heights. Similarly divergent duct with Reynolds number 50,000 (D-5B) with bottom surface rib attachment shows fig. 10 rib height 9 mm is higher heat transfer enhancement compared to others. In general the divergent duct with 9 mm rib height is always higher heat transfer enhancement due the recirculation and decelerations of fluid flow.

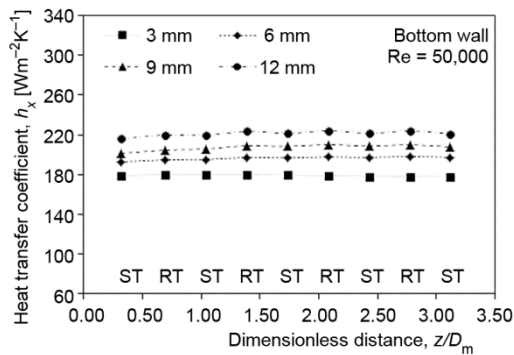


Figure 9. Variation of local heat transfer coefficient for channels with different rib heights, convergent (C-5B)

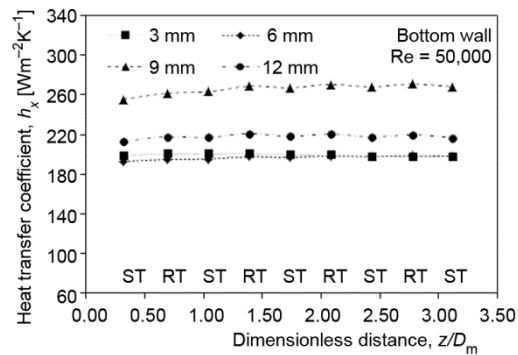


Figure 10. Variation of local heat transfer coefficient for channels with different rib heights, divergent (D-5B)

Variation of thermo-hydraulic performance parameter convergent and divergent ducts

Figure 11 shows the variation of thermo-hydraulic performance parameter with Reynolds number for different channel configurations presently tested in convergent duct. The values of Nu and *f* from the smooth channel at Re = 20,000 is considered as the baseline reference values. Hence the thermo-hydraulic performance (THP) parameter showed a value of unity for this case. THP values for the smooth converged channel increases with increase in the Reynolds number and this indicates that this channel performs better at higher Reynolds number. All ribbed channels also showed an increased values of THP with the Reynolds number. However, compared to the smooth channel, only the channel with 3 mm rib height (*e*) showed THP values greater than the smooth channel and other channels showed THP values lesser than the smooth channel. This indicates that the converged channels with rib heights larger than 3 mm are not showing an overall good performance when compared to the smooth channel. Even though there may be a heat transfer enhancement with these channels (*e* > 3 mm), this positive is nullified by the increased pressure drop across those channels. It must be noted that the converged channel with rib height of 3 mm show THP parameter values very close to that of the smooth channel, particularly at higher Reynolds number. The highest value of THP parameter for the ribbed channel with *e* = 3 mm is 2.62 which could be interpreted that this ribbed channel at Re = 60,000 is 262% better than the smooth channel at Re = 20,000.

The values of Nusselt number obtained from the experiments were compared with the standard correlation. Dittus-Boelter correlation for estimating the Nusselt number for the smooth ducts of uniform cross-section from the inlet to the outlet is defined by:

$$Nu_o = 0.023 Re^{0.8} Pr^{0.4} \tag{14}$$

To find the friction factor for smooth pipes using:

$$f_o = 0.0791 \text{ Re}^{-0.25} \quad (15)$$

Figure 12 show the variation of thermo-hydraulic performance parameter with the Reynolds number for different channel configurations presently tested in divergent duct. The THP parameter showed a value of unity for the smooth channel at $\text{Re} = 20,000$, whose values are considered as the baseline reference. THP values for the smooth convergent channel increases with increase in Re and this indicates that this channel performs better at higher Reynolds number. The highest value of THP parameter for the ribbed channel with $e = 3 \text{ mm}$ is 4.40 which could be interpreted that this ribbed channel at $\text{Re} = 60,000$ is better than the smooth channel at $\text{Re} = 20,000$.

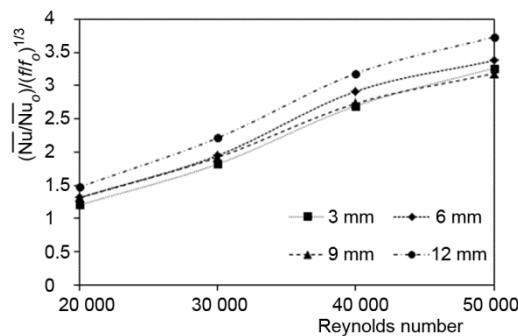


Figure 11. Variation of thermo-hydraulic performance factor with different Reynolds number, divergent channel

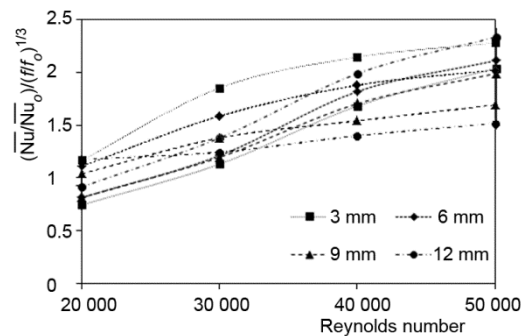


Figure 12. Variation of thermo-hydraulic performance factor with different Reynolds number, convergent channel

Friction factor

The friction factor across the domain is plotted in fig. 13 which is a dimensionless number since it is the ratio of the effective pressure drop across the convergent channel and the kinetic head of the mean velocity. The value of f is found to be decreasing with increase in Reynolds number from 20,000 to 30,000. Any further increase in Reynolds number does not change the value of f and the trend is horizontal. This indicates that the increased pressure drop with increased Reynolds number is compensated by the increased kinetic head in the denominator of f . It is to be noted that the velocity increases with increased Reynolds number and this contributes to the almost constant value of f . With increase in rib height the value of f is found to increase and this is due to the larger pressure drop values in the numerator of f for the given Reynolds number. The friction factor across the domain is plotted in fig. 14 which is a dimensionless number since it is the ratio of the effective pressure drop across the divergent channel and the kinetic head of the mean velocity. The value of f is found to be decreasing with increase in Reynolds number similar to the convergent channels.

Comparison between maximum heat transfer enhancement and optimum pressure drop in 3 mm convergent and divergent duct

Figure 15 exhibits stream wise turbulent intensity in dimensionless distance with heat transfer coefficient for 3 mm convergent and divergent duct with Reynolds number

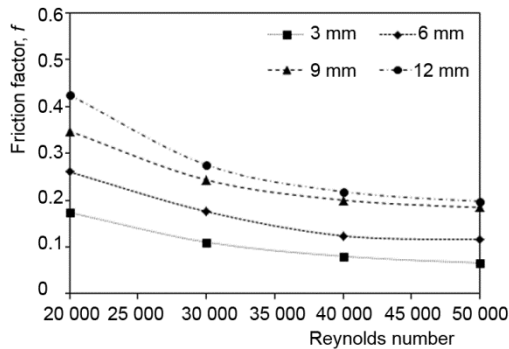


Figure 13. Variation of friction factor across the channel for all rib heights at different Reynolds number, divergent channel

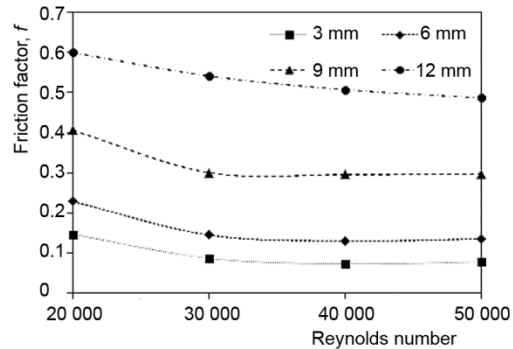


Figure 14. Variation of friction factor across the channel for all rib heights at different Reynolds number, convergent channel

various from $20 \cdot 10^3$ to $50 \cdot 10^3$. The graph shows 3 mm rib height divergent duct for 50,000 Reynolds number (D-5B) with bottom rib attachment reaches maximum heat transfer coefficient $190 \text{ W/m}^2\text{K}$ in between 2nd and 3rd rib position It happens because of large number recirculation air and flow separation will take place.

Sometimes, large adverse pressure gradient causes back flow that create zone with more disorder flow. On the other hand, after a big separation the flow impinges on the wall just before the rib and creates a high pressure zone with little recirculation. Primary part of re-circulation zone in case of ribs height 3 mm, is characterized by more regular measurement values compared to secondary re-circulation zone. Thus it is possible to differentiate flow separation zone from re-attachment zone.

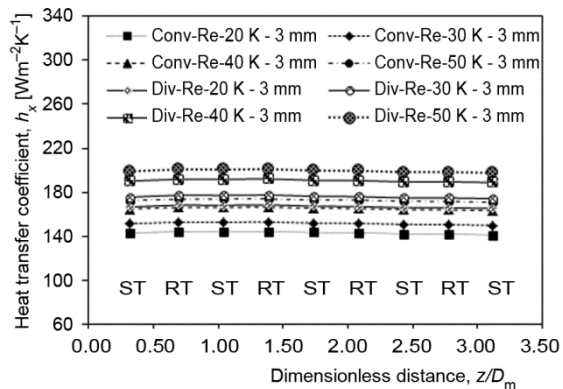


Figure 15. Comparison between 3 mm rib height convergent – divergent duct

Conclusions

The article analyses an experimental study of local heat transfer and friction factor of a convergent/divergent rectangular duct with inclination angle of 1° in y-direction for different (3, 6, 9, and 12 mm) height square ribbed ducts. The local heat transfer coefficient and the pressure recover factor were measured for air flowing in the divergent, convergent duct with different height square ribs. The Reynolds number variation range was $2 \cdot 10^4$ to $5 \cdot 10^4$.

The experimental set-up was fabricated and flow, thermal characteristics were tested by measuring wall temperature at selected locations, fluid temperature at the inlet and the outlet and wall static pressures at the channel inlet and the outlets. Ribbed channels show larger pressure drops than the smooth channels and the value of pressure drop increases with increase in rib height. This can be attributed to the recirculation zones in the downstream side of each rib.

With increase in rib height the strength and size of this recirculation zone increases and hence the pressure drop increases with increase in rib height. Channel with 3 mm ribs

showed negligible increase in pressure drop compared to the smooth channel as the influence of recirculation zones behind the 3 mm ribs might be small.

The friction factor f is found to be decreasing with increase in Reynolds number from 20,000 to 30,000. Any further increase in Reynolds number does not change the value of f and the trend is horizontal. The highest value of THP parameter for the ribbed convergent channel with $e = 3$ mm is 2.62 which could be interpreted that this ribbed channel at $Re = 50,000$ is 262% better than the others.

Compared to the convergent channels, the pressure drop values for the corresponding geometry configuration and the given flow Reynolds number were found to be lower. This indicates that the pressure drops in the divergent channels are lesser than the convergent channels. The highest value of THP parameter for the ribbed divergent channel with $e = 3$ mm is 3.5 which could be interpreted that this ribbed channel at $Re = 50,000$ is better than others. Based on the thermo-hydraulic performance parameter; divergent duct with 3 mm rib height gives maximum heat transfer and minimum pressure drop compared to other rib heights and channels.

Nomenclature

A – surface area, [m²]
 $A(x)$ – surface area from inlet to the position of x , [m²]
 C_p – pressure recovery factor
 c_p – heat capacity, [J Kg⁻¹ K⁻¹]
 D_h – hydraulic diameter, [m]
 D_m – average hydraulic diameter (= 86 mm)
 e – rib height
 f – friction factor
 f_o – fanning friction factor for the smooth duct
 h – heat transfer coefficient, [Wm⁻²K⁻¹]
 k – thermal conductivity, [Wm⁻¹K⁻¹]
 L – axial length of duct, [m]
 m – mass flow rate, [kgs⁻¹]
 Nu – Nusselt number
 Nu_o – Nusselt number for the smooth duct
 \bar{Nu} – average Nusselt number
 Δp – pressure drop of duct, [Nm⁻²]
 Q – heat transfer rate, [W]
 Q_{loss} – heat loss to the environment, [W]
 Re – Reynolds number
 Re_m – Reynolds number based on D_m

RT – rib thermocouple
 ST – surface thermocouple
 T – temperature, [K]
 T_b – local bulk temperature of air
 T_w – wall temperature, [K]
 U_m – cross-section average streamwise velocity, [ms⁻¹]
 x – streamwise direction

Greek symbols

α – orientation of the rib, [°]
 λ – parameter defined by eq. (11)
 ρ – density of the coolant, [kgm⁻³]

Subscripts

b – bulk
 loss – heat loss
 m – mean
 in – inlet
 out – outlet
 w – wall temperature
 x – local

References

- [1] Abuaf, N., Kercher, D. M., The Heat Transfer and Turbulence in a Turbine Blade Cooling Circuit, *ASME Journal of Turbomachinery*, 116 (1994), 1, pp. 169-177
- [2] Han, J. C., Park, J. S., Developing Heat Transfer in Rectangular Channel with Rib Turbulators, *International Journal of Heat Mass Transfer*, 31 (1988), 1, pp. 183-195
- [3] Han, J. C., Heat Transfer and Friction Characteristics in Rectangular Channels with Rib Turbulators, *Journal of Heat Transfer*, 110 (1988), 2, pp. 321-328
- [4] Wagner, J. H., et al., Heat Transfer in Rotation Serpentine Passages with Trips Normal to the Flow, *Journal of Turbomachinery*, 114 (1992), 4, pp. 847-857
- [5] Johnson, B. V., et al., Heat Transfer in Rotating Serpentine Passages with Trips Skewed to the Flow, *Journal of Turbomachinery*, 116, (1994), 1, pp. 113-123
- [6] Johnson, B. V., et al., Effect of Rotation on Coolant Passage Heat Transfer, *NASA Contractor Report No. 4396*, NASA Contractor, Washington, USA, 1993

- [7] Chen, Y., *et al.*, Detailed Mass Transfer Distribution in a Ribbed Coolant Passage, *International Journal of Heat Mass Transfer*, 43 (2000), 8, pp. 1479-1492
- [8] Bo, T., *et al.*, Developing Buoyancy Modified Turbulent Flow in Ducts Rotating in Orthogonal Mode, *Journal of Turbomachinery*, 117, (1995), 3, pp. 474-484
- [9] Lacovides, H., The Computation of Flow and Heat Transfer through Rotating Ribbed Passage, *International Journal of Heat Fluid flow*, 19 (1988), 5, pp. 393-400
- [10] Sivakumar, K., *et al.*, Heat Transfer and Pressure Drop Comparison between Smooth and Different Sized Rib – Roughened Divergent Rectangular Ducts, *International journal of Engineering and Technology*, 6 (2014), 1, pp. 263-272
- [11] Sivakumar, K., *et al.*, Influence of Rib Height on Heat Transfer Augmentation – Application to Aircraft Turbines, *International Journal of Turbo Jet Engines*, 31 (2014), 1, pp. 87-95
- [12] Qantani, M. A., *et al.*, A Numerical Study of Flow and Heat Transfer in Rotating Rectangular Channels (AR = 4) with 45° Rib Turbulators by Reynolds Stress Turbulence Model, *Journal of Heat Transfer*, 125 (2003), 1, pp. 19-26
- [13] Wang, L. H., *et al.*, Experimental Study of Developing Turbulent Flow and Heat Transfer in Ribbed Convergent/Divergent Square Duct, *International Journal of Heat and fluid flow*, 22 (2001), 6, pp. 603-613
- [14] Rongguang J., *et al.*, Heat Transfer Enhancement in Square Ducts with V-Shaped Ribs of Various Angles, *Proceedings, ASME Turbo Expo, Power for Land, Sea and Air, Amsterdam, The Netherlands, Vol. 3, 2002*, pp. 469-476
- [15] Chandra, P. R., *et al.*, Heat Transfer and Friction Behaviours in Rectangular Channels with Varying Number of Ribbed Walls, *International Journal of Heat and Mass Transfer*, 46 (2003), 3, pp. 481-495
- [16] Amro, M., *et al.*, An Experimental Investigation of the Heat Transfer in a Ribbed Triangular Cooling Channel, *International Journal of Thermal Science*, 46 (2007), 5, pp. 491-500
- [17] Abhishek, G., *et al.*, Local Heat Transfer Distribution in a Square Channel with 90° Continuous, 90° Saw Tooth Profiled and 60° Broken Ribs, *Experimental Thermal and Fluid Science*, 32 (2008), 4, pp. 997-1010
- [18] Thianpong, C., *et al.*, Thermal Characterization of Turbulent Flow in a Channel with Isosceles Triangular Ribs, *International Communication in Heat and Mass Transfer*, 36 (2009), 7, pp. 712-717
- [19] Julker, Md. N., *et al.*, Turbulence and Pressure Drop Behaviours around Semicircular Ribs in a Rectangular Channel, *Thermal Science*, 18 (2014), 2, pp. 419-430
- [20] Caliskan, S., Baskaya, S., Experimental Investigation of Impinging Jet Array Heat Transfer from a Surface with V-Shaped and Convergent-Divergent Ribs, *International Journal of Thermal Science*, 59 (2012), Sep. pp. 234-246
- [21] Abdulrazzaq, T., *et al.*, Numerical Simulation on Heat Transfer Enhancement in Channel by Triangular Ribs, *Int. J. of Mech. Aerospace Industrial Mechanotronic and Manufacturing Engineering*, 7 (2013), 8, pp. 49-53
- [22] Sriharsha, V., *et al.*, Influence of Rib Height on the Local Heat Transfer Distribution and Pressure Drop in a Square Channel with 90° Continuous and 60° V-Broken Ribs, *Applied Thermal Engineering*, 29 (2009), 11-12, pp. 2444-2456
- [23] Sjerić, M., *et al.*, Development of a Two Zone Turbulence Model and its Application to the Cycle-Simulation, *Thermal Science*, 18 (2014), 1, pp. 1-16
- [24] Bakić, V., *et al.*, Experimental Investigation of Turbulent Structures of Flow around a Sphere, *Thermal Science*, 10, (2006), 2, pp. 97-112.
- [25] Kline, S. J., McClintock, F. A., Describing Uncertainties in Single Sample Experiments, *Mechanical Engineering*, 75 (1953), 1, pp. 3-8
- [26] Moffat R. J., Describing the Uncertainties in Experimental Results, *Experimental Thermal Fluid Science*, 1 (1988), 1, pp. 3-17
- [27] Box, G. E. P., *et al.*, *Statistics for Experimenters*, John Wiley and Sons, New York, USA, 1978, pp. 453-509